Dynamic Response Analysis of Storage Cask Lid Structure Subjected to Lateral Impact Load of Aircraft Engine Crash

Belal Almomani[a], Sanghoon Lee[b], Hyun Gook Kang[a*]
aDept. of Nuclear and Quantum Engineering, KAIST, 291 Daehak-ro, Yuseong-gu, Daejeon 305-701, Korea
bDept. of Mechanical and Automotive Engineering, Keimyung University, Daegu, Korea
*Corresponding author: hyungook@kaist.ac.kr

1. Introduction

Dry storage casks are widely used, as more and more long-term storage of spent nuclear fuel is required. Metal storage cask may prove to be a safe solution, which can be used as a multi-purpose system such as for transportation and storage. Risk assessment of spent fuel storage is an important area in the nuclear safety field. Calculating the leakage rate of radionuclides under extensional hypothetical accident conditions, which would exceed the design requirements of the dual-purpose metal cask (DPMC), is one of the essential elements of the risk assessment.

Several numerical methods and tests have been carried out to measure the capability of storage cask to withstand extreme impact loads [1-6]. Testing methods are often constrained by cost, and difficulty in preparation for several impact conditions with different applied loads, and areas of impact. Instead, analytic method is an acceptable process that can easily apply different impact conditions for the evaluation of cask integrity.

The aircraft engine impact is considered as one of the most critical impact accidents on the storage cask that significantly affects onto the lid closure system and may cause a considerable release of radioactive materials.

This paper presents a method for evaluating the dynamic responses of one upper metal cask lid closure without impact limiters subjected to lateral impact of an aircraft engine with respect to variation of the impact velocity. The calculation of the relative macroscopic dynamic displacements between the cask flange surface and lid closure was conducted by non-linear dynamic finite element analyses using LS-DYNA [7]. This analysis is an interface between the mechanical behavior of the cask system under impact loads and its radiological consequences analysis.

2. Finite Element Model of Cask System

The considered cask model in this study consists of a forged carbon steel body closed by one upper bolted lid closure as a containment boundary. The internal structures such as canister and spent fuel basket are replaced by a dummy weight that has the same mass and similar stiffness to achieve the correct package weight. This model is free-standing on a concrete pad modeled as a rigid body fixed to the ground as illustrated in Fig.1. The aim of this model is to analyze the macroscopic dynamic response of the lid closure system and to calculate sliding and opening displacements between the lid and the flange. Therefore, unnecessary details of the cask system are omitted in the modeling.
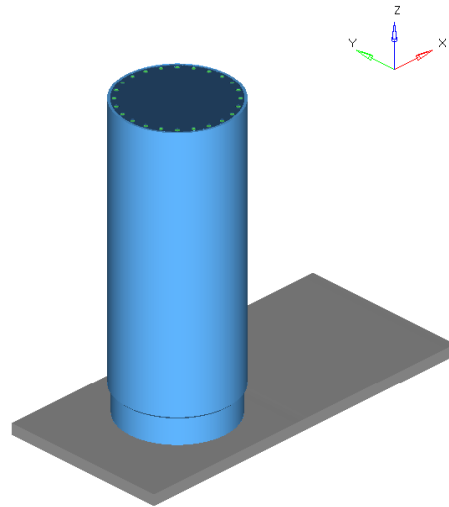
Fig. 1. Finite-element model of the simplified storage cask assembly.

The design specification of the cask system is described in Table I.

Table I: Design specification of the cask model

Part	Design features
Cask outer body	Outer Diameter (O.D): 2.1 m Inner Diameter (I.D): 1.656 m Thickness: 22 cm Height: 5.4 m Total weight: 97 ton
Lid	Thickness: 20.1 cm Diameter: 2.01 m Weight: 4.9 ton
Bolts	Number of bolts: 24 Length: 27.9 cm Diameter: 4.8 cm
Dummy solid body	Diameter: 1.65 m Height: 4.845 m Weight: 33.7 ton

The finite element model includes 955,939 nodes, and 869680 linear hexagonal elements with material type defined by using the keyword *MAT_PIECE_LINEAR_PLASTICITY. Table II lists the material properties of the principal components employed in the impact analysis.

Table II: Material properties of the cask model

Part	Mass density (Kg/m³)	Young's modulus (MPa)	Poisson's ratio	Yield stress (MPa)
Cask body	7850	210000	0.3	334.92114
Dummy	3253	200000	0.3	322.48584
Bolts	7850	206000	0.3	835.72668
Lid	7850	210000	0.3	334.92114

3. Analysis Assumptions and Methodology to Calculate Lid Displacements

The selected impact scenario in this study is a large commercial aircraft engine penetrates the wall of a storage facility through local fracture and hits horizontally the top part of the free-standing cask, which is the most realistic scenario and expected to produce a serious damage to the containment boundary of the cask body. Large turbofan engine type (CF6-80C2), used for B747-400, was chosen since it covers a high range of possible mechanical impact. The engine weight is about 4.4 tons, turbo fan diameter is 2.7 m, the length is 4.3 m, and has a blunt nose shape (shape factor 0.84). [8]

3.1 Impact Velocity Range

Analytical estimation for the local perforation of interim storage concrete wall building subjected to the relevant jet engine has been studied [9]. Modified NDRC formula and Degen formula have been used to predict the perforation depth and to define the concrete wall thickness criteria due to engine impact [10]. Based on the existing design concepts for interim storage buildings, the wall thickness is around 0.7 to 1.2 m [11]. The probable conceivable values of impact velocity during abnormal landing caused by a malfunction or an intentional attack would be around (50~200 m/s) for B747-400. Fig. 2 shows the relationship between the impact velocity and the perforation depth for reinforced concrete with compressive strength of 13.8 MPa predicted by Degen formula using the design specification of the CF6-80C2 jet engine.
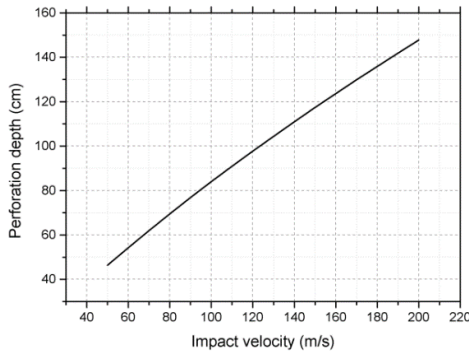
Fig. 2. The relationship between the impact velocity and the perforation depth for CF6-80C2 jet engine, with Degen reduction factor 0.6. [10]

Then, the residual velocity after penetrating the storage wall facility of the relevant jet engine can be estimated by using the following Pétry formula [12]:

$$v_{res} = v_{imp} \sqrt{1 - (0.5b / H)} \qquad (1)$$

Where v_{res} is the residual velocity for the jet engine, b is the thickness of the building wall, and H is depth of the perforation. Fig. 3 shows the relationship between the residual impact velocities with respect to the possible impact velocities onto various wall thicknesses.
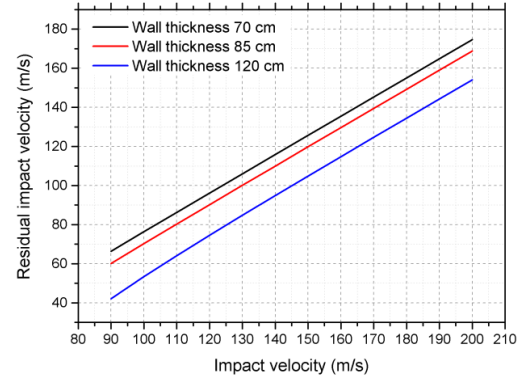
Fig. 3. The relationship of the initial impact velocity with the reduced impact velocity.

The selected reference concrete wall thickness for the storage facility is 85 cm. Therefore, the possible values of reduced impact velocity after perforating 85 cm concrete wall would be around (60~165 m/s). Nevertheless, only four impact velocities 60, 90, 120, 150 m/s were selected because of the linear relationship between the impact velocity with the perforation depth and residual velocity. Thus, selecting a small number of impact velocities will be a good enough insight to evaluate the lid closure response for this case study.

3.2 Impact Load Function

For this analysis, the impact load-time history function and effective loading contact area for the relevant aircraft engine are needed. However, this paper will not discuss the derivation of the load-time function since many literatures gave enough information about analytical approaches to estimate loadings resulting from a direct aircraft crash onto a hypothetical rigid or soft target. The Riera's method has been widely used in the aircraft impact research and it is appropriate for a simplified impact simulation [13]. Therefore, the impact load-time history curve proposed by CRIEPI [1] based on the Riera's method for the relevant aircraft engine at impact velocity 60 m/s was used as a reference impact load curve due to lacking of information for the structure of the jet engine. Furthermore, load curves for different impact velocities were derived based on the reference load curve with applying Riera iterative algorithm from the following equation:

$$F(t) = ma + \mu[x(t)]v(t)^2 \qquad (2)$$

Where a is deceleration from destruction of the B747-400 which is equal 29.98 m/s^2 [14], m is the missile (engine) mass, $\mu(x(t))$ is the mass per unit length at location x and $v(t)$ is the impact velocity of uncrushed portion of engine. In addition, a rational assumption to linearly scale down the reference time of the relevant engine impact was applied for a purpose of drawing the load curves for various higher impact velocities based on the momentum equation. For instance, the time reduction factor for impact velocity 60 m/s to 120 m/s equals two. This means, the time duration of the engine crash at impact velocity 120 m/s is double faster than the engine crash at impact velocity 60 m/s. Fig. 4 shows the impact force time-history curves.
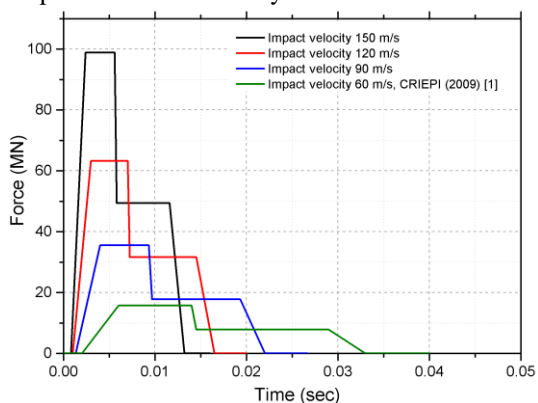
Fig. 4. Impact load-time history for the GE/CF6-80C2 FE engine model at impact velocities 60, 90, 120, and 150 m/s.

The effective impact diameter of the circular area with considering the mass and stiffness distribution of the CF6-80C2 engine is about 1.4 m [1], which applied on the analysis model of the lateral impact as seen in Fig. 5. The impact loads are uniformly distributed on 1639 representative nodes on the cask model.
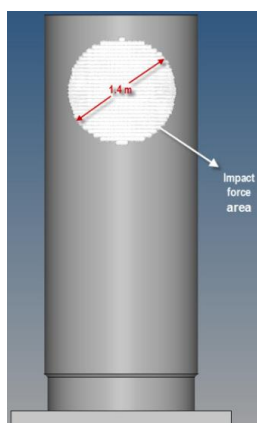
Fig. 5. Analysis model for aircraft engine impact on the storage cask.

3.3 Contact Interactions

The modeling of contact interactions between the interfaces of each part is carried out by activating general contact commands available in LS-DYNA.

A sliding contact between the flange surface and the lid with constant static fraction coefficient of 0.2 was assumed and for all other interior contact surfaces of the cask body [15]. As long as the cask body and lid are much stiffer than the closure bolts, thereby the bolt tightening force does not greatly affect on the lid movements due to large impact loads. Therefore, the initial pretension of the lid bolts caused by a preload tightening torque is neglected as a more conservative.

3.4 Analysis Model Description

One upper node on the lid and one lower node on the cask body of eight locations were selected for tracking the dynamic displacements during the impact. The node locations are near where the O-ring would be located to evaluate the actual leak area between the O-ring and the flange surface. The node movements can be in perpendicular direction as opening displacement and parallel direction as sliding displacement with respect to the cask flange surface. Fig. 6 illustrates the directions of the opening and sliding displacements. From the displacement time histories, the amount of separations between the cask body and lid can be determined, and the accumulative relative sliding displacements $D_{Accumulated}$ can be defined as shown in Fig. 7.
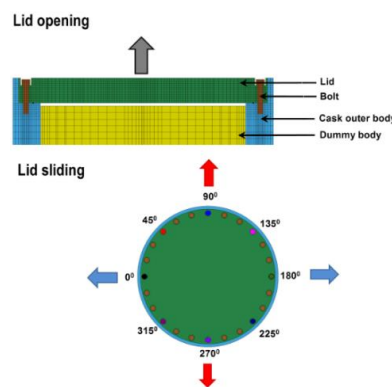
Fig. 6. Definition of opening and sliding displacement of the lid.
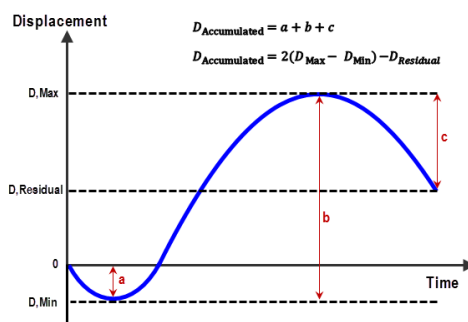
Fig. 7. The definition of the accumulated relative sliding displacement [1].

4. Results and Discussion

In this section, the results of the impacts specified in the previous section are addressed in order to obtain a reasonable maximum opening and sliding displacements of the upper lid. Fig. 8 shows the behavior of the displacement contour from the beginning to 0.05 seconds of the simulation at impact

velocity 60 m/s. This simulation time is enough to predict the possible maximum displacement values.
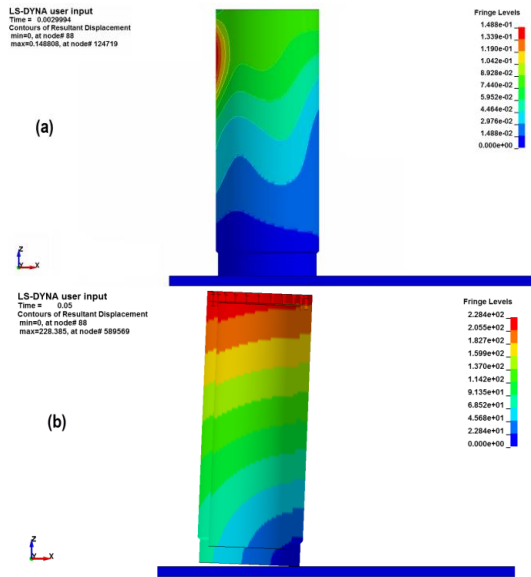
Fig. 8. Result displacement contour at impact velocity 60 of the simplified metal cask model; a) at the moment of impact 0.003 sec, b) at the end of the simulation time 0.05 sec.

Fig. 9 and 10 show the time history of the opening and sliding displacements during the lateral impact hitting the top part of the cask at eight positions around the lid for various impact velocities.

As can be seen from Fig. 9 and 10, the continuous fluctuation response is caused by lack of friction and material damping within the finite element model. In reality, the surface friction will cause these fluctuations to stop quickly. Therefore, this study is concern on the maximum possible displacements to be a more conservative approach. Generally, it is observed from the figures that when the impact loads increases the closure opening and sliding is also increases. Moreover, large sliding deformations of the lid were generated in the all impact velocity ranges, while opening deformations were relatively smaller. However, the opening displacements at different locations around the lid pattern are considered as the major factor of generating opening gaps, which may cause a permanent failure of the seal and the lid might be to lose the leak-tightness.

Regarding the sliding displacement, it is presumed that there is no leakage path due to parallel movements of the lid in this study. However, in reality shock parallel movements of the lid, which exceed some certain values such as defined by BAM criteria [16], may cause scratches on the sealing surface cask or break the O-ring seals that would generate a significant amount of leakage. Table III shows the summary of the maximum possible accumulated sliding displacements and Fig. 11 illustrates the pattern of accumulated sliding movements. In this study, the $D_{Accumulated}$ consequences are not contributing in the calculation of leak gap area.
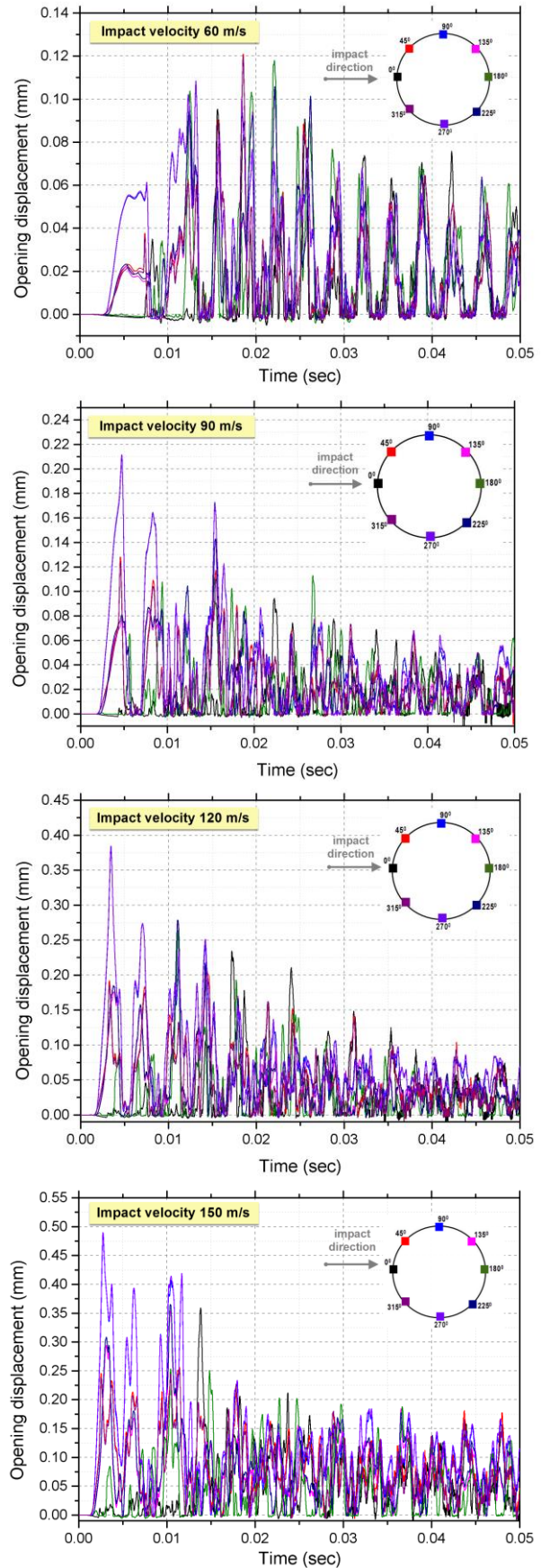
Fig. 9. Time history of lid opening displacements at eight locations for impact velocities 60, 90, 120, and 150 m/s.
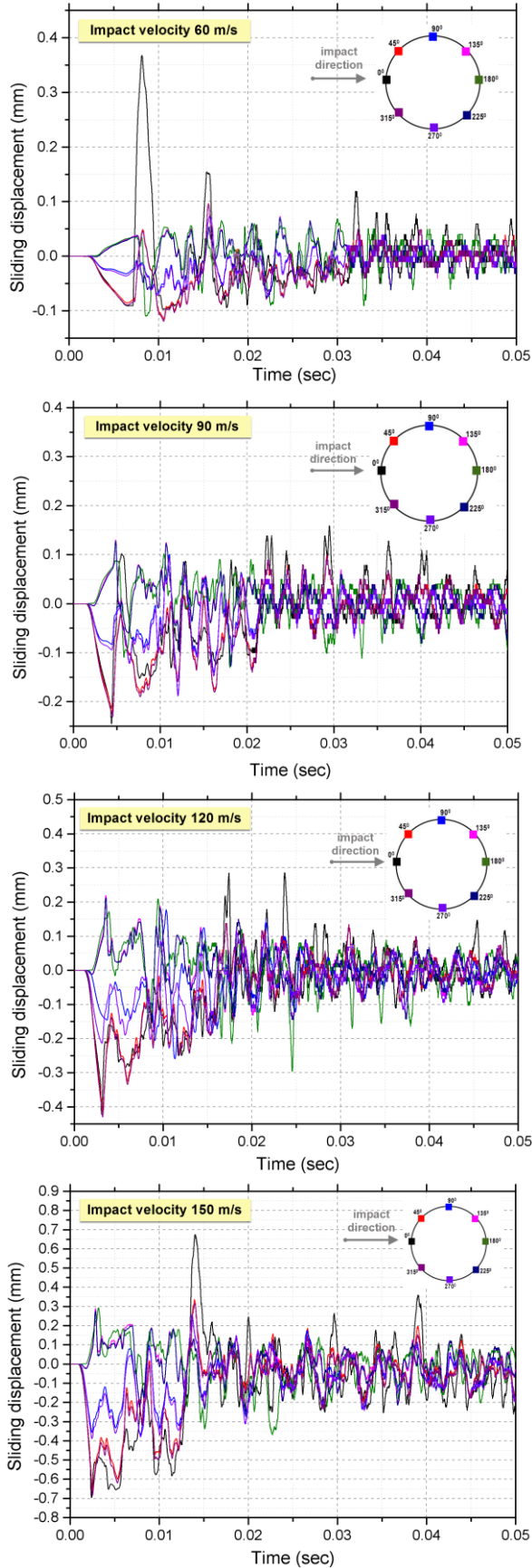
Fig. 10: Time history of lid sliding displacements at eight locations for impact velocities 60, 90, 120, and 150 m/s.

Table III: Summary of accumulated sliding displacements of the impact analyses

Node location	The maximum accumulated displacement (mm)			
	60 m/s	90 m/s	120 m/s	150 m/s
0º	0.931	0.727	1.445	2.961
45º	0.434	0.621	1.133	2.172
90º	0.307	0.590	0.875	1.427
135º	0.325	0.560	0.747	1.076
180º	0.329	0.554	0.971	1.305
225º	0.317	0.579	0.723	1.160
270º	0.307	0.58	0.711	1.465
315º	0.44	0.631	1.165	2.183
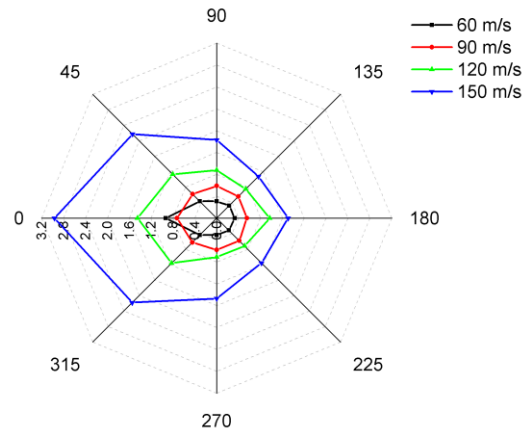
Fig. 11. Pattern of accumulated sliding displacements for the lid closure.

It is noted from Fig. 11; the maximum accumulated displacement at the node location 0º in case of impact velocity 60 m/s is higher than the generated maximum accumulated displacement for impact velocity 90 m/s. The reason of this surprising result is due to the effects of many factors on the closure sliding. For instance, when applying a high dynamic impact load on the cask body the external frequency and damping ratio will be very high. Moreover, the storage cask system has a heavy weight. Thus, the dynamic magnification factor (DMF) is less than one and the system is not able to respond probably because it is not getting enough time for responding; as a result, the dynamic displacement will be less. From this special case, low dynamic impact load may cause higher sliding displacements for lid closure.

Table IV shows a summary of the maximum possible opening displacements for the eight locations on the lid during the moment of impact load effect and the maximum generated opening displacements after the engine totally crash on the cask body and the impact load becomes zero. The shaded values in Table IV are the maximum opening displacements at each node location along the time displacement history. These values at the initial moment of the impact can be used for evaluating the pre-compression of the O-ring seals to check if the O-ring can recover these opening distances or not.

Table IV: Summary of seal region displacements of the impact analyses

| Node location | Maximum opening displacement (mm) | | | | | | | |
| | During the impact load effect | | | | After the impact load effect | | | |
	60 m/s (0-0.033 sec)	90m/s (0-0.022 sec)	120 m/s (0-0.0165 sec)	150 m/s (0-0.0132 sec)	60 m/s (0.033-0.05 sec)	90 m/s (0.022 -0.05 sec)	120 m/s (0.0165-0.05 sec)	150 m/s (0.0132-0.05 sec)
0°	0.095	0.051	0.105	0.048	0.075	0.094	0.234	0.359
45°	0.12	0.128	0.213	0.256	0.064	0.069	0.154	0.215
90°	0.107	0.209	0.381	0.483	0.054	0.072	0.153	0.227
135°	0.103	0.142	0.274	0.353	0.063	0.077	0.169	0.184
180°	0.118	0.112	0.264	0.253	0.067	0.113	0.193	0.251
225°	0.105	0.143	0.279	0.365	0.063	0.073	0.166	0.178
270°	0.108	0.211	0.384	0.490	0.056	0.075	0.154	0.233
315°	0.119	0.123	0.199	0.252	0.064	0.073	0.162	0.226

Table V: Calculated closure area sizes

| Impact velocity (m/s) | Maximum leak path area (mm^2) | |
	During the impact load effect	After the impact load effect
60	38.76 at time 0.0123 sec	27.63 at time 0.03883 sec
90	64.42 at time 0.01555 sec	26.74 at time 0.02689 sec
120	98.9 at time 0.01112 sec	60.07 at time 0.01788 sec
150	148.63 at time 0.0104 sec	74.67 at time 0.0179 sec

While the opening displacements, after the impact load effects becomes zero, can be considered as the permanent opening gaps if the initial maximum opening displacement exceeds the recovery distance of O-ring. Then these values might be used for calculating the amount of radioactive release rate.

The resulting of leakage area from opening displacement can be determined from the generated geometric shape with a height of the opening displacements for two nodes and a width of the selected bolt spacing 69 cm. By scanning all the time history displacements for the eight nodes, the maximum leak area can be found at a specified time during and after the effect of impact load in the simulation. Table V summarizes the maximum leak area calculations for the four impact analyses. These leak area calculations were determined without taking into account the influence of the pre-compression O-ring seal. According to the NR-6672 [17], the typical large O-ring can recover any opening distance up to 2.5 mm. Therefore, it is noticed that the generated opening displacements are very small in all impact cases compared to the O-ring recovery distance. This happened due to the fact that only a small portion of the impact energy is absorbed by the deformation of cask system, while the rest of energy are translated into the kinetic energy of the cask; as a result, the center of gravity of the cask was moved horizontally and vertically in the direction of the engine impact. Thus, further research is needed for analysis the effect of the global dynamic behavior of the free-standing storage cask on the lid closure after the lateral impact caused by jet engine.

3. Conclusions

An assessment method to predict damage response due to the lateral engine impact onto metal storage cask has been studied by using computer code LS-DYNA.

The dynamic behavior of the lid movements was successfully calculated by utilizing a simplified finite element cask model, which showed a good agreement with the previous research. The simulation analyses results showed that no significant plastic deformation for bolts, lid, and the cask body. In this study, the lid opening and sliding displacements are considered as the major factors in initiating the leakage path.

This analysis may be useful for evaluating the instantaneous leakage rates in a connection with the sliding and opening displacements between the lid and the flange to ensure that the radiological consequences caused by an aircraft engine crash accident during the storage phase are within the permissible level. This method is somewhat a conservative representation of the aircraft impact and it would address some of the uncertainties in the assessment.

REFERENCES

[1] K. Shirai, K. Namba, and T. Saegusa, Safety Analysis of Dual Purpose Metal Cask Subjected to Impulsive Loads due to Aircraft Engine Crash, Journal of Power and Energy Systems, Vol.3, pp.72-82, 2009.
[2] G. Wieser, L. Qiao, H. Völzke, D. Wolff, and B. Droste, Safety Analysis of Casks Under Extreme Impact Conditions, Packaging and Transportation of Radioactive Materials Conference, No.208, 2004.
[3] J.H. Yoon, W.S. Choi, S. Lee, and K.S. Seo, Arising technical issues in the development of a transportation and storage system of spent nuclear fuel in Korea. Nuclear Engineering and Technology, Vol.43, pp.413-420, 2011.
[4] B. Droste, H. Völzke, G. Wieser, and L. Qiao, Safety Margins of Spent Fuel Transport and Storage Casks Considering Aircraft Crash Impact, Radioactive Materials Transport and Storage Conference, Vol. 13, No. 3-4, pp.313-316, 2002.
[5] S. Lee, W.S. Choi, K.Y. Kim, J.E. Jeon, K.S. Seo, Impact Analyses and Tests of Metal Cask Considering Aircraft Engine Crash, Annual Waste Management (WM) Conference, 2012.

[6] G. Marchaud, L. Vilela, S. Nallet, Designing a Radioactive Material Storage Cask against Airplane Crashes with LS-DYNA, 3th International LS-DYNA Users Conference, 2014.

[7] LS-DYNA Computer Program, Version R7.1.1, Livermore Software Technology Corporation.

[8] http://www.geaviation.com/commercial/engines/cf6/

[9] B. Almomani, M. Yoo, H.G. Kang, Development of Aircraft Impact Scenario on a Concrete Cask in Interim Storage Facility, Proceeding of Korean Nuclear Society Spring Conference, 2015.

[10] NEI 07-13, Revision 8P, Methodology for Performing Aircraft Impact Assessments for New Plant Designs, Washington, DC; 2011.

[11] B. Thomauske, Realization of the German Concept for Interim Storage of Spent Nuclear Fuel – Current Situation and Prospects, Annual Waste Management (WM) Conference, 2003.

[12] G. Ben-Dor, A. Dubinsky, T. Elperin, Empirical Models for Predicting Protective Properties of Concrete Shields Against High-Speed Impact, Journal of Mechanics of Materials and Structures, Vol. 8, No. 2-4, 2013.

[13] J. D. Riera, On the Stress Analysis of Structures Subjected to Aircraft Impact Forces, Nuclear Engineering and Design, pp.415-426, 1968.

[14] V. Iliev, K. Georgiev, V. Serbezov, Assessment of Impact Load Curve of Boeing 747-400, Journal of science, techniques and innovations for the industry "Machines, Technologies, Materials", 2011.

[15] U. Zencker, L. Qiao, M. Weber, E. Kasparek, H. Völzke, Reliability of Cask Designs under Mechanical Loads in Storage Facilities, Probabilistic Safety Assessment and Management PSAM 12 Conference, 2014.

[16] G. Wieser, L. Qiao, A. Eberle, H. Völzke, Thermo-Mechanical Finite Element Analyses of Bolted Cask Lid Structures, 14th International Symposium on the Packaging and Transportation of Radioactive Materials PATRAM, 2004.

[17] US-NRC, Reexamination of Spent Fuel Shipment Risk Estimates, NUREG/CR-6672, Vol. 1, 2000.